

L-/M-cone opponency in visual evoked potentials of human cortex

Mirella Telles Salgueiro Barboni

Department of Experimental Psychology,
University of Sao Paulo, Brazil
Department of Ophthalmology,
Semmelweis University, Budapest, Hungary



Balázs Vince Nagy

Department of Experimental Psychology,
University of Sao Paulo, Brazil
Department of Mechatronics,
Optics and Engineering Informatics,
Budapest University of Technology and
Economics, Budapest, Hungary

Cristiane Maria Gomes Martins

Department of Experimental Psychology,
University of Sao Paulo, Brazil

Daniela Maria Oliveria Bonci

Department of Experimental Psychology,
University of Sao Paulo, Brazil
Instituto Israelita de Ensino e Pesquisa Albert
Einstein, Sao Paulo, Brazil

Einat Hauzman

Department of Experimental Psychology,
University of Sao Paulo, Brazil
Instituto Israelita de Ensino e Pesquisa Albert
Einstein, Sao Paulo, Brazil

Avinash Aher

Department of Ophthalmology,
University Hospital Erlangen, Germany

Tina I. Tsai

Department of Ophthalmology,
University Hospital Erlangen, Germany

Jan Kremers

Department of Ophthalmology,
University Hospital Erlangen, Germany

Dora Fix Ventura

Department of Experimental Psychology,
University of Sao Paulo, Brazil
Instituto Israelita de Ensino e Pesquisa Albert
Einstein, Sao Paulo, Brazil

L and M cones send their signals to the cortex using two chromatic (parvocellular and blue–yellow koniocellular) and one luminance (magnocellular) pathways. These pathways contain ON and OFF subpathways that

respond to excitation increments and decrements respectively. Here, we report on visually evoked potentials (VEP) recordings that reflect L- and M-cone driven increment (L_i and M_i) and decrement (L_D and

Citation: Barboni, M. T. S., Nagy, B. V., Martins, C. M. G., Bonci, D. M. O., Hauzman, E., Aher, A., Tsai, T. I., Kremers, J., & Ventura, D. F. (2017). L-/M-cone opponency in visual evoked potentials of human cortex. *Journal of Vision*, 17(9):20, 1–12, doi:10.1167/17.9.20.



M_D) activity. VEP recordings were performed on 12 trichromats and four dichromats (two protanopes and two deuteranopes). We found that the responses to L_I strongly resembled those to M_D , and that L_D and M_I responses were very similar. Moreover, the lack of a photoreceptor type (L or M) in the dichromats led to a dominance of the ON pathway of the remaining photoreceptor type. These results provide electrophysiological evidence that antagonistic L/M signal processing, already present in the retina and the lateral geniculate nucleus (LGN), is also observed at the visual cortex. These data are in agreement with results from human psychophysics where M_I stimuli lead to a perceived brightness decrease whereas L_I stimuli resulted in perceived brightness increases. VEP recording is a noninvasive tool that can be easily and painlessly applied. We propose that the technique may provide information in the diagnosis of color vision deficiencies.

Introduction

Light stimulation, using “spectral compensation” or “silent substitution” methods allow the independent modulation of a single photoreceptor type (Estévez & Spekrijse, 1974, 1982; Kremers, 2003). For instance, L or M cones can be selectively stimulated so that the downstream neural activity is driven uniquely by the L or by the M photoreceptor types. Similarly, stimuli that emphasize photoreceptor excitation onset or offset, such as the luminance increments (rapid-on) or decrements (rapid-off) sawtooth stimulus profiles can be used to evoke activity driven by ON and OFF subprocesses, respectively. In the present study, we used the silent substitution stimulation method to isolate L- and M-cone responses combined with cone excitation increments (ON) or decrements (OFF) using sawtooth modulation profiles.

In trichromatic subjects, L-cone driven electroretinogram (ERG) responses to rapid-on excitation increments (i.e., ON stimuli) resemble responses recorded with rapid-on luminance increments that are driven by both (L and M) types of photoreceptors. Similarly, L-cone driven decrements (rapid-off stimulation) elicited ERGs resembling luminance OFF responses (for the rapid-on and -off white stimulation, see Barboni et al., 2013; for cone-isolated rapid-on and -off stimulation, see Kremers et al., 2014; McKeefry et al., 2014; Tsai et al., 2016). In addition, L-cone driven responses to full field sinusoidal stimuli have larger amplitudes than those elicited by M-cone isolating full field stimuli (Jacob et al., 2015), indicating that the retina is L-cone dominated in most trichromatic subjects.

Another interesting observation is that L-cone driven increment (L_I) ERG responses bear resemblance to M-cone driven decrement (M_D) responses. Similarly, ERG responses to L_D and to M_I display peaks and troughs with similar amplitudes and implicit time (Kremers et al., 2014; McKeefry et al., 2014; Tsai et al., 2016). This aligns well with the L/M cone opponency in the parvocellular pathway, the earliest visual substrate for the perception of the red–green chromatic contrast. Furthermore, recent investigations on visual perception using L- or M-cone selective stimuli showed that the M-cone increments are perceived as a brightness decrement by subjects with normal color vision, whereas L-cone increments were perceived as brightness increments (Parry, McKeefry, Kremers, & Murray, 2016).

In the retina, cone increment and decrement responses are processed by distinct pathways mediated by bipolar cells with different types of membrane receptors, which are depolarized or hyperpolarized by a cone excitation change (Kaneko, 1973; Werblin & Dowling, 1969). However, it is not completely known how these retinal signals are processed by the brain.

The purpose of the study was to examine if the increments and decrements are processed in the visual cortex just as in the ERG recordings and in the psychophysical experiments. Because both these techniques revealed similarities between L- and M-cone signals of opposite polarities, the working hypothesis for the present study was that cortical processing recorded by the VEPs (an intermediate level between retinal and psychophysical responses) will also be able to reveal similar opponent processes.

We found that visually evoked potentials (VEPs) of L- and M-cone increments (ON; L_I and M_I) were quite different from each other. Similarly, L- and M-cone decrements (OFF; L_D and M_D) have shown dissimilar VEPs. However, in agreement with our hypothesis, L- and M-cone responses of opposite polarity resembled each other (i.e., L_I responses resembled M_D VEPs, whereas M_I and L_D VEP were similar).

Materials and methods

Participants

The experiments adhered to the tenets of the Declaration of Helsinki and were approved by the ethics committee of the University Hospital, University of São Paulo, Brazil (CEP-HU/USP 156.826). Signed informed consent was obtained from each subject after explanation of the nature and possible consequences of the study. The inclusion criteria were: best-corrected visual acuity of 20/20, absence of ophthalmological

diseases as well as of any other disease that could affect the visual system. Participants were 16 volunteers: 12 trichromatic (mean age 20 ± 7 years), two protanope (21 and 23 years old), and two deuteranope (33 and 39 years old), whose color vision deficiency was confirmed genetically (see the following). Color vision phenotype of all subjects was determined by the Cambridge Colour Test (CCT; Regan, Reffin, & Mellon, 1994). See Table 1 for results of the CCT.

Genetic analysis

An analysis of the visual pigment genes was performed to confirm the psychophysical color vision classification of the dichromats. DNA samples were extracted from the buccal brush using the Gentra Puregene Buccal Cell Kit (Gentra Systems, Inc., Minneapolis, MN). To evaluate the presence of L or M genes on the X chromosome, a genetic test was performed according to Neitz and Neitz (1995). Exons 2, 3, and 4 of the genes were amplified with polymerase chain reaction (PCR) and the PCR products were sequenced to evaluate the presence of polymorphisms in the genes. PCRs were carried out using High Fidelity Platinum Taq Polymerase, 10× High Fidelity Buffer, $MgCl_2$ (Invitrogen, Carlsbad, CA), 10mM GeneAmp dNTPs (Applied Biosystems, Inc., Foster City, CA) and 20 mM primers (Invitrogen) in 50 μ L reactions. The primers used and the PCR conditions were the same as described by Neitz et al. (2004). PCR products were visualized by electrophoresis in 1.0% agarose gel and purified with Illustra GFX™ PCR DNA and Gel Band Purification Kit (GE Healthcare, Little Chalfont, Buckinghamshire, UK). The PCR products were directly sequenced in both directions with BigDye® Terminator v3.1 Cycle Sequencing Kit (Applied Biosystems) and the 3500 Applied Biosystems Sequencer. Electropherograms were visualized and aligned in BioEdit v7.0.9.0 (Hall, 1999).

VEP recordings

The pupil was dilated with a drop of mydriaticum (0.5% tropicamide). VEP responses were acquired from one randomly chosen dilated eye (other eye was covered by a patch) using gold cup skin electrodes placed on the scalp according to the International 10/20 system (American Clinical Neurophysiology, 2006). The active electrode was in position Oz. The reference electrode was placed in position Fz and the ground electrode was placed on the forehead. The impedances between all electrodes were below 5 k Ω . The signals were amplified 100,000×, filtered between 1 and 300

Subject	Age	CCT*			
		Protan	Deutan	Tritan	
1	Control	16	29	29	38
2	Control	14	52	61	69
3	Control	26	33	33	40
4	Control	27	29	30	65
5	Control	13	49	33	90
6	Control	13	73	71	79
7	Control	13	36	46	62
8	Control	13	37	46	52
9	Control	29	41	29	52
10	Control	27	36	26	53
11	Control	27	42	29	54
12	Control	25	39	30	69
	AVE	20	41	39	60
	St dev	7	12	14	15
13	deuteranope	39	325	953	68
14	protanope	21	752	99	45
15	deuteranope	33	282	469	78
16	protanope	23	658	184	64

Table 1. Demographic information of the population showing age and the result of the Cambridge Colour Test (CCT) considered to classify the subjects. *CCT: psychological computerized test that allows to estimate color discrimination thresholds along the protan, deutan, and tritan axes from a central achromatic point in the CIE 1976 $u'v'$ color space. Results are given as the 10^4 x distance between the chromaticity of the threshold and the central point (chromaticity of the background; Regan, Reffin, & Mollon, 1994).

Hz, and sampled at 1024 Hz using the RetiPort system (Roland Consult, Brandenburg, Germany). At least 20 episodes, each lasting 1 s, were averaged. The first 2 s of each episode were discarded to avoid onset artifacts.

Visual stimulation

Light stimulation was provided by a Super Color Ganzfeld Q450SC (Roland Consult) equipped with six arrays of light-emitting diodes (LEDs) of different colors. As previously described (Kremers et al., 2014; Tsai et al., 2016), the stimuli were developed to provide triple silent substitution conditions for the L- or M-cones. Briefly, four light-emitting diode types were activated: red (peak wavelength \pm full width at half maximum: 638 ± 9 nm), green (523 ± 19 nm), blue (469 ± 11 nm), and amber (594 ± 8 nm). Mean luminance, stimulus temporal profile, modulation depth, phase, and temporal frequency of each LED were independently controlled by the RETiport software. The luminance of each of the four primaries LED arrays was modulated with rapid-on and rapid-off sawtooth luminance profiles (Table 2). It allowed the

LED	Peak wavelength (nm)	Full width at half maximum	Mean luminance (cd/m ²)* / contrast (%)		Modulation profile			
			L-cone isolation**	M-cone isolation**	LI	LD	MI	MD
Red	638	± 9	80 / 90	80 / 90	Rapid-ON	Rapid-OFF	Rapid-OFF	Rapid-ON
Green	523	± 19	40 / 7	40 / 23	Rapid-ON	Rapid-OFF	Rapid-OFF	Rapid-ON
Blue	469	± 11	4 / 1	4 / 2	Rapid-OFF	Rapid-ON	Rapid-ON	Rapid-OFF
Amber	594	± 8	160 / 25	160 / 60	Rapid-OFF	Rapid-ON	Rapid-ON	Rapid-OFF

Table 2. Characteristics of the four LEDs used and the light stimulation for each protocol. *Total mean luminance (284 cd/m²) and mean chromaticity ($x = 0.5686$, $y = 0.3716$; CIE 1931 color space) were the same for all four stimulus condition; **L- and M-isolation provided 18% and 17% of modulation contrasts, respectively.

rods to be unmodulated in stimuli in which either the excitation of the L cones or the excitation of the M cones was rapidly incremented or decremented.

The mean luminance (284 cd/m²) and the mean chromaticity ($x = 0.5686$, $y = 0.3716$; CIE 1931 color space), and thus the state of adaptation, was the same for all stimulus conditions. The scotopic retinal illuminance, calculated from the scotopic spectral sensitivity of the eye (rods) and the stimulus spectral distribution, was approximately 5600 scot Td considering 8 mm pupil diameter and the photopic retinal illuminance was 14275 Td. It was previously shown that in ERG measurements rod isolating stimuli (25% rod contrast) did not elicit significant rod driven responses above about 400 Td (Maguire et al., 2016). Therefore, rod-driven signals are negligibly small. L and M isolation provided very similar contrasts: 18% and 17% of modulation contrast, respectively. The tests were performed in a dark room (lower than 10^{-4} cd/m² photopic luminance).

L or M cones were stimulated with a 4 Hz sawtooth temporal modulation of cone excitation in two conditions: rapid-on (increments) and rapid-off (dec-

rements). Each increment cycle consisted of an abrupt increment in cone excitation, to activate the ON mechanism, followed by a linear decrease in excitation. Decrement profiles were the opposite, to activate the OFF mechanism (see Tsai et al., 2016 for the description of the visual stimulation).

The characteristics of the stimuli for each protocol are shown in Table 2. The stimuli allowed independent control of rod, L-, M-, and S-cone photoreceptor outputs, defined as the Michelson contrast around a mean excitation.

Data analysis

Peak and trough analysis and fast Fourier transformation (FFT) were applied to the signals in order to obtain the amplitude and implicit time/phase responses. In the time domain analysis, the implicit times of three components (N1, P1, and N2; see Figure 2C for definitions) were measured. The amplitude of the N1 component was defined as the difference between the signal at the sudden excitation change in the stimulus

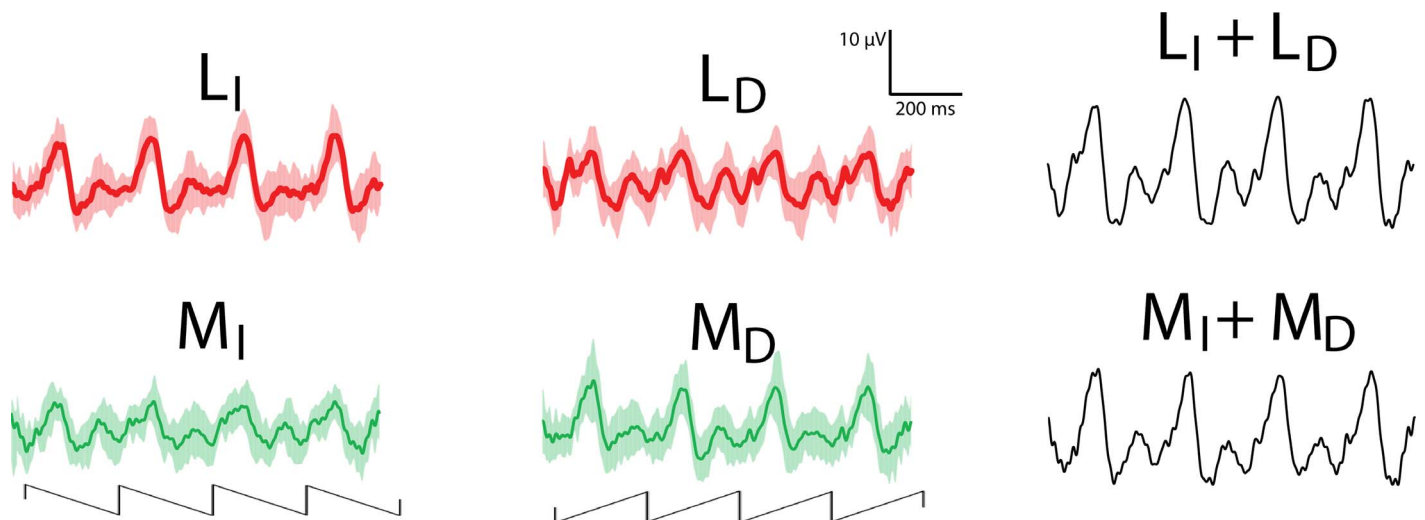


Figure 1. Averaged (\pm one standard deviation; shaded area) responses ($N = 12$) to four stimulus cycles obtained for each protocol, as well as the sum of the average signals (right column).

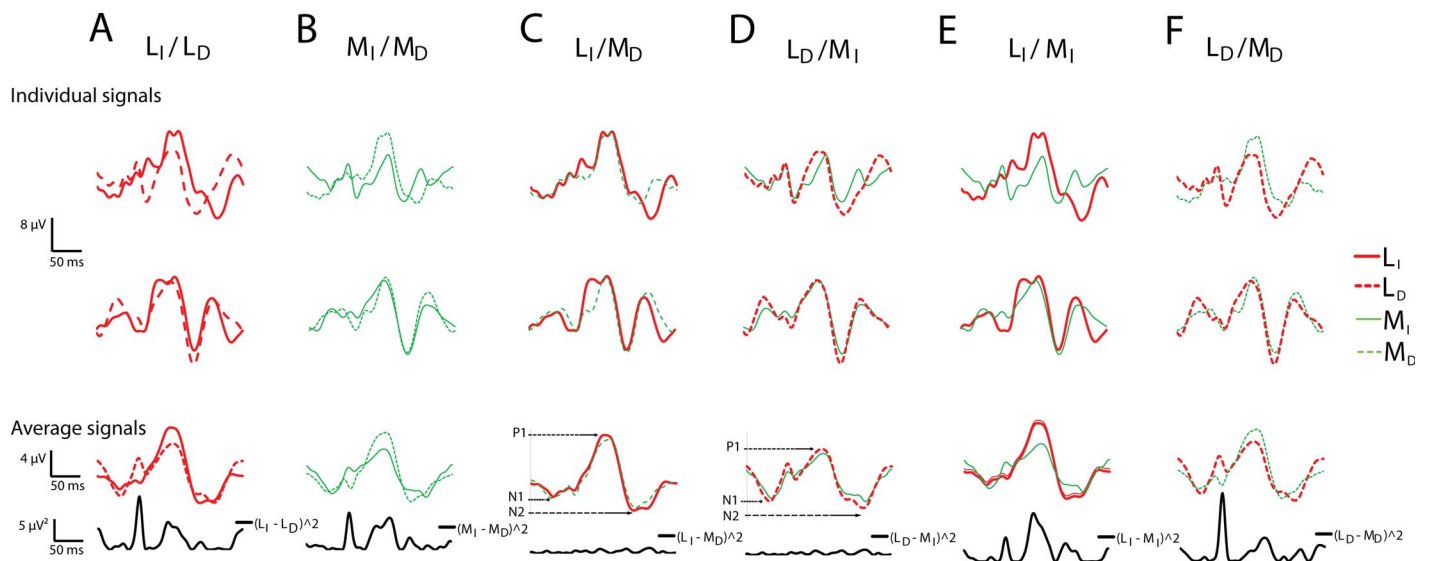


Figure 2. Signals of two typical subjects (upper and middle rows). The average signals of 12 healthy subjects for each cone-isolated condition (L_I , L_D , M_I , and M_D) are shown as follows. Red-thicker traces represent the L-cone and green-thinner traces the M-cone isolated responses (continuous = increment and dotted = decrement). The black bold traces represent the squared distances between the two signals at each instant. A and B show the comparison between increment and decrement responses driven by the same cone type. In the middle, the L_I with M_D (C) and L_D with M_I (D) are compared. The last two columns are the comparisons between L- and M-increments (E) and L- and M-decrements (F). The upper scale is related to the individual signals. The lower scales are related to the average signals (upper) and to the squared distance (lower).

(baseline) to the minimum of the component (typically between 20 and 60 ms after the sudden excitation change). The P1 amplitude was defined as the voltage difference between the minimum of the N1 to the peak of the P1 component (within a time window between 100 and 150 ms after the sudden change in cone excitation). Finally, the N2 amplitude was measured as the voltage difference between the P1 peak and the subsequent N2 minimum (typically between 180 and 220 ms after the sudden excitation change). Comparisons were performed using Student's t test, after verifying the normality of the parameter distribution (Shapiro–Wilk test). Pearson's correlation was calculated to analyze the relationship between the different stimulus conditions.

Results

Figure 1 shows the average (\pm one standard deviation; shown as the shaded area) response of the trichromatic subjects ($N = 12$) for the four conditions: L- and M-cone driven responses are shown in the upper and lower rows respectively. Each signal displays the response to four stimulus cycles. Left and middle columns display the response to increments and decrements respectively. The right columns display the addition of increment and the decrement signals (rapid-on + rapid-off). The additions give a visualization of

the asymmetry between ON and OFF mechanisms (Pangeni, Lämmer, Tornow, Horn, & Kremers, 2012). The additions are large and similar for L- and M-cone driven VEPs indicating similar ON-OFF asymmetries. Furthermore, the L_I responses were similar to the M_D responses and the L_D and M_I responses resembled each other.

The responses were further analyzed by measuring amplitudes and implicit times of the first negative component (N1), the positive component (P1), and the second negative wave (N2). For this analysis, the responses to the four cycles, as shown in Figure 2, were further averaged to obtain the response to a single cycle. Due to large response variability between subjects (sometimes some components could not be observed) the time domain analysis was occasionally difficult. Therefore, we also conducted a frequency domain analysis, in order to obtain the amplitudes and phases of the first (4 Hz) and the second (8 Hz) harmonics.

The averaged responses to one stimulus cycle are shown in Figure 2. Increment and decrement selective cone-driven responses were superimposed in A and B in order to compare their time to peak values and amplitudes. Although the troughs and peaks occur at similar times, there are profound differences between the two (visualized by the thick traces below the responses that show the squared distances at each instant). The major L_D positivity is somewhat smaller than that of L_I . Furthermore, the L_D response displays

t-test	LI-MD	MI-LD	LI-MI	LD-MD
LI-MD	-	0.29	0.03	0.05
MI-LD		-	0.0008	0.02
LI-MI			-	0.27
LD-MD				
AVE	200	172	362	457
STDEV	150	175	258	513

Table 3. Statistic comparison between the sums of the squared distances.

a secondary positivity preceding the peak that is larger than in the L_I response. Figure 2B shows that M_I and M_D responses differ in a similar manner as the L-cone driven responses, however, in an opposite manner: the M_I response displays a smaller main peak but a larger secondary peak in comparison with the M_D response. The thick traces below the averaged responses display the squared distances between the increment and decrement responses to visualize systematic differences between the two. Obviously, the differences between the two were similar for L- and M-cone isolating stimuli. The sum of squared distances was calculated for each subject to quantify the overall difference between the responses. They were 434 and 338 μV^2 , on average, for M_I-M_D and for L_I-L_D responses, respectively.

Figure 2C and 2D show the comparison between L_I and M_D and between L_D and M_I , respectively. Here, the peaks and troughs occur at the same time with similar amplitudes and the responses are generally very similar as it is also shown by the squares of the differences, which show only minor deviations from zero. The sum of the squared distances was 200 and 172

μV^2 , on average, for the L_I-M_D comparison and for the M_I-L_D comparison, respectively.

Figure 2E and 2F show the comparison between L and M responses, respectively of each type, increment (left) and decrement (right), in order to show the differences between the two (also visualized by the squared distances given as thick traces as follows). The sum of the squared distances was 362 and 457 μV^2 , on average, for the L_I-M_I comparison and for the L_D-M_D comparison, respectively. Table 3 shows the statistical comparisons of the sum of squared distances. Observe that in the comparisons with the sum of squared distances between L_I-M_D and with L_D-M_I , they were significantly higher ($p < 0.05$).

Figures 3 and 4 show the correlations between amplitudes and phases of the first and second harmonic response components obtained in the different conditions from the 12 trichromatic subjects. In agreement with the results shown above, the first and second harmonic amplitudes of L_I and M_D responses (Pearson's $r = 0.8$; $p = 0.002$ and $r = 0.6$; $p = 0.03$, respectively) and of L_D and M_I responses (Pearson's $r = 0.7$; $p = 0.02$ and $r = 0.8$; $p = 0.004$, respectively; Figures 3 and 4; upper graphs) were positively correlated. First and second harmonic L_D and M_I response phases (lower graphs) also showed a significant positive correlation (Pearson's $r = 0.9$; $p = 0.001$ and $r = 0.9$; $p < 0.001$). The phases of L_I and M_D show a tendency of correlation; we would expect this to be statistically significant at higher test result numbers. The other components were not significantly correlated.

Figure 5 shows the averaged responses of the control group (upper traces), similar to the lower graphs of Figure 2, and the individual responses of four dichromatic (two protanopic and two deuteranopic)

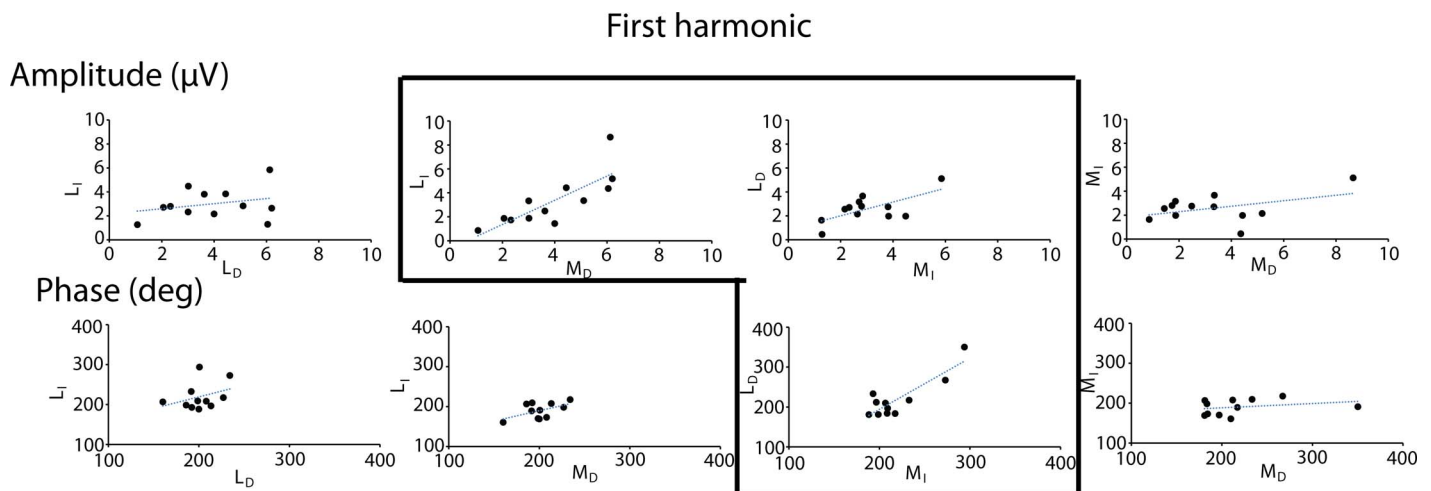


Figure 3. Comparisons between amplitudes (upper graphs) and phases (lower graphs) of first harmonic response components. The correlations are shown for the comparison of $L_I \times L_D$ (left graphs), $M_I \times M_D$ (right graphs), and of $L_I \times M_D$ (second column) and $L_D \times M_I$ (third column). The enclosed area indicates significant correlations: $L_I \times M_D$ (Pearson's $r = 0.8$; $p = 0.002$) and $L_D \times M_I$ (Pearson's $r = 0.7$; $p = 0.02$) response amplitudes, and $L_D \times M_I$ (Pearson's $r = 0.9$; $p = 0.001$) response phases.

Second harmonic

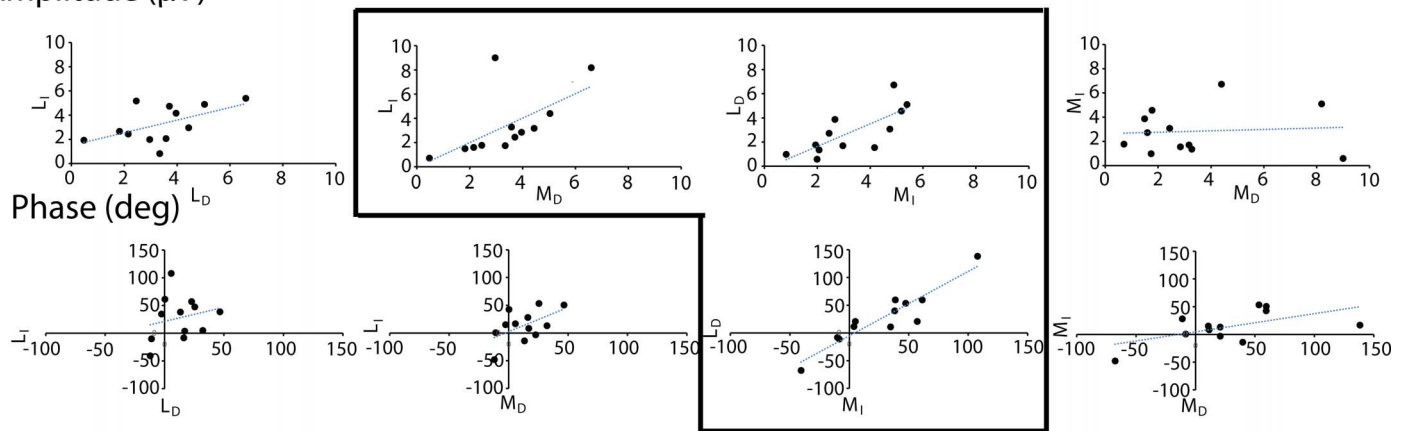
Amplitude (μV)

Figure 4. Comparisons between amplitudes (upper graphs) and phases (lower graphs) of second harmonic response components. The correlations are shown for the comparison of $L_I \times M_D$ (left graphs), $M_I \times M_D$ (right graphs), and of $L_I \times M_D$ (middle-left graphs) and $L_D \times M_I$ (middle-right graphs). The enclosed graphs show significant correlations: $L_I \times M_D$ (Pearson's $r = 0.6$; $p = 0.03$) and $L_D \times M_I$ (Pearson's $r = 0.8$; $p = 0.004$) response amplitudes, and $L_D \times M_I$ (Pearson's $r = 0.9$; $p < 0.001$) response phases.

subjects. The genetic analysis of these subjects showed the presence of only one copy of the L-opsin gene and no M-opsin gene in the two deuteranope subjects. One protanope had one M-opsin gene and no L-opsin gene. No polymorphisms in the L- or the M-opsin genes were found. The other protanope subject had two copies of the M-opsin gene and no L-opsin gene, and one of the M copies had polymorphisms in the exon 2.

Similar to Figure 2, we plotted L_I together with M_D , and L_D together with M_I responses. Unlike the responses of the color normal subjects, the L_I and M_D responses were not similar in the dichromatic subjects. Also the L_D and M_I responses were different. In both cases, the responses to stimulation of the nonpresent cones were very small. Interestingly, we found a smaller response to L_D in the deuteranope subjects and of the M_D in the protanope subjects. Only the increment responses (rapid-ON) after isolation of the present cone type were large.

Discussion

Subcortical areas of the visual system, such as the retina (Diller et al., 2004; Lee, Martin, & Grünert, 2010) and the lateral geniculate nucleus (LGN; Derrington, Krauskopf, & Lennie, 1984; Lennie, Krauskopf, & Sclar, 1990; Zeki, 1973), are composed of different groups of cells that are differently activated by the retinal photoreceptor types. The L and M cone types, for instance, provide principal input to the L/M opponent (through the midget bipolar and midget ganglion cells in the retina and the parvocellular cells in

the LGN) and to the luminance (via diffuse bipolar and parasol ganglion cells in the retina and the magnocellular cells in the LGN) pathways. Although subcortical processing of information by these pathways is fairly well understood, it is generally not well understood how signals from the isolated L and M cone types are subsequently translated in the visual cortex.

In the present study we recorded VEPs while presenting light stimuli that isolate L-cone or M-cone activity to increments (rapid-on) or decrements (rapid-off) of cone excitations. We were able to show that L/M-cone opponency initiated by the photoreceptors in the retina (DeValois & DeValois, 1993), recently recorded in human ERGs using cone-isolated stimuli (Kremers et al., 2014; McKeefry et al., 2014; Tsai et al., 2016), and found in visual perception (Giulianini & Eskew, 1998; Parry et al., 2016; Sankeralli & Mullen, 2001), is also measurable using VEP. L_I and M_D cortical responses resemble each other, as do L_D and M_I responses. Moreover, the lack of a photoreceptor type (L or M) leads to a domination of the other photoreceptor type as recorded in the cortical responses in dichromats.

The simplest explanation of the similarity of the responses to M- and L-cone sawtooth stimuli of opposite polarity is the involvement of L/M-cone opponency as is found in the parvocellular subcortical pathway. VEP responses probably receive input from parvo- and magnocellular pathways when using luminance stimuli of different contrasts (Rudvin & Valberg, 2006). Thus, it is not unlikely that the VEPs mainly represent parvocellular activity with cone-isolating stimuli. Interestingly, the resemblance between L_I and M_D and between L_D and M_I responses in the VEPs is

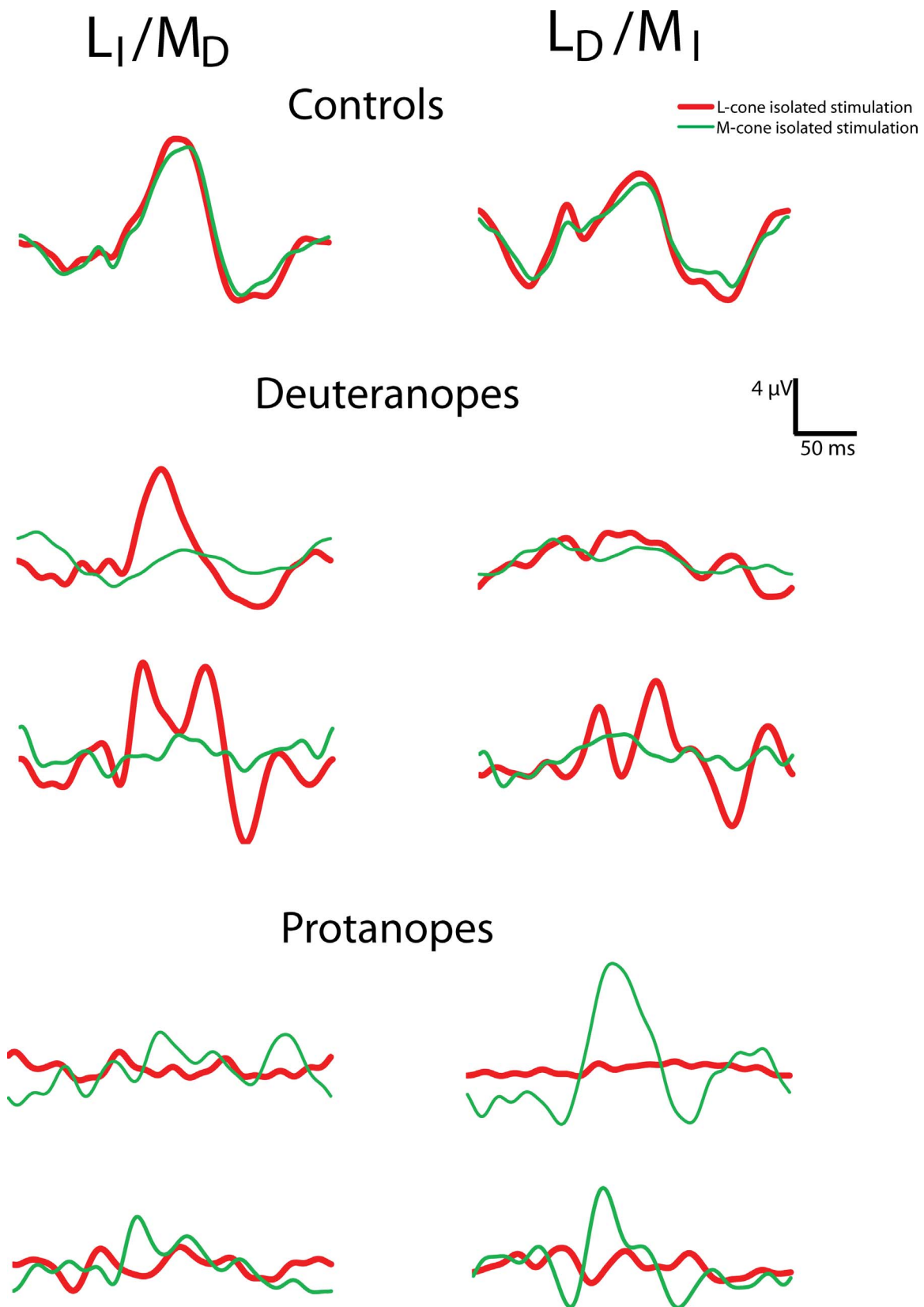


Figure 5. Average responses of the control group ($N = 12$; upper traces) and individual responses of two deuteranopic (middle traces) and two protanopic (lower traces) subjects. In the dichromatic subjects responses to stimulation of the lacking cone type leads to a relatively negligible response. Moreover, they displayed mainly increment responses of the preserved cone type: The deuteranopic subjects showed higher L_I responses compared with the L_D responses and the protanopic subjects displayed normal M_I responses and reduced M_D responses.

present with full field stimuli. The resemblances in ERGs was clearer when the stimuli were not full field but spatially restricted to the central 70° of the retina (Tsai et al., 2016). ERG responses to L- and M-cone isolating stimuli can indeed be explained by a mixture of luminance and chromatic responses. However, when the stimuli are restricted to the central retina the chromatic responses strongly dominate (Tsai et al., 2016). Owing to the cortical magnification of the foveal responses, we can explain why the full field VEPs also are dominated by the chromatic responses.

L-cone ERG responses have larger amplitudes compared with the M-cone ERG responses (Kremers & Pangeni, 2012; Kremers et al., 2014; McKeefry et al., 2014; Tsai et al., 2016). This may be due to the larger number of midget bipolar cells with direct L-cone inputs (Brainard et al., 2000). This was not observed in the VEPs: L- and M-cone stimulation result in similar amplitude responses only with different polarity. This is expected when the responses are dominated by parvocellular signals, where the L/M ratio is known to be more balanced (Kremers, Lee, & Kaiser, 1992; Smith, Lee, Pokorny, Martin, & Valberg, 1992).

The responses to luminance modulation may be explained by an asymmetry in the ON- and OFF-subpathways. In the L/M cone opponent pathway, there are four subpathways: +L–M, +M–L, –L+M, –M+L. The ON-/OFF-asymmetry could explain response differences between +L–M and +M–L on the one hand and –L+M and –M+L on the other hand. However, an additional asymmetry between +L–M and +M–L and between –L+M and –M+L must be assumed; otherwise, their responses would cancel each other out. Which mechanisms are responsible for these signals is an important open question. A possible source of asymmetry may be attributed to the L/M cone ratio. There generally are more L than M cones, and thus there are probably also more postreceptoral neurons belonging to the +L–M than to +M–L subpathways. Similarly –L+M neurons probably outnumber –M+L neurons. If the answer lies in the relative numerosity of +L–M compared with +M–L cells then it can be expected that the signals as measured in the ERGs are also transmitted to the cortex because the imbalance in cell numbers is possibly also reflected in an imbalance in the numbers of cortical cells. Although this may be a sound basis for a proposed model, it is still at a qualitative stage, and further work is needed to consider the many parameters that should be part of a quantitative model (such as L/M ratio as a function of retinal eccentricity; individual differences in L/M ratio; quantitative contributions of the different postreceptoral pathways to mass potentials such as the ERG or the VEP, etc.).

We speculate that there is an increasing interaction of the chromatic opponent mechanisms initiated with

neural signals from each L or M cone in subcortical areas that might be responsible for the nonlinearity of the signal at the level of the primary visual cortex. The contribution of the present study is that these observations might be taken into account when modeling the origins of the human VEP.

In the primate visual cortex there are different classes of neurons processing specific characteristics of visual information. Similarities and dissimilarities have been noted regarding chromatic-opponent cells in the visual cortex compared with those in the retina and in the LGN. Complex cells (Hubel & Wiesel, 1968), color cells (Dow, 1974; Dow & Gouras, 1973; Gouras, 1970), double-opponent cells (Johnson, Hawken, & Shapley, 2001), and other types of visual cortical cells are considered to be the neurons responsible for chromatic processing. Like the midget bipolar and ganglion cells of the retina (see a review by Lee et al., 2010) and the chromatic cells of the LGN (Hubel & Wiesel, 1966; Wiesel & Hubel, 1966), these cortical cells receive antagonistic inputs from the different types of photoreceptors. The L/M opponency in VEP signals indicates that the opponent cell responses dominate the VEP responses. This is in agreement with data from functional magnetic resonance imaging (fMRI) where the BOLD (blood-oxygen-level dependent) signal suggests that the neural activity in the visual cortex is strongly driven by L/M-cone opponent inputs (Engel, Zhang, & Wandell, 1997).

In the present study we chose an intermediate temporal frequency of 4 Hz. ERG responses at lower temporal frequencies to L- or to M-cone isolated sawtooth stimulation did not display additional features. L- and or M-cone stimulation up to about 12 Hz has been associated with responses driven by chromatic opponent postreceptoral mechanisms (Kremers & Pangeni, 2012). We assumed that the 4 Hz stimulation used in the present study might activate mainly the midget bipolar cells that send their signals to the parvocellular pathway and, subsequently, to the chromatic opponent cells of V1. Furthermore, frequencies below 4 Hz are much more contaminated by lower frequency noise, such as blinks and eye movements that usually happen during the recordings of flicker stimulation (Kremers, Rodrigues, Silveira, & da Silva-Filho, 2010; Pangeni et al., 2012).

The method used here was suitable to record cortical responses using L- and M- cone isolated stimuli in subjects with normal color vision and also in dichromats. Interestingly, the M_I responses in the protanopes and the L_I responses in the deutanopes were similar to each other (see Figure 5), indicating that these signals are processed similarly in these subjects and are luminance driven (since these subjects lack L/M opponent pathways that is observed in the VEPs of the trichromats). The stimulation of the lacking cone type

leads to a negligible response and the decrement responses were smaller (though clearly present in two dichromats). The smaller response to decrement stimulation (OFF-response) of the L-cone isolated stimulus in deuteranope subjects and of the M-cone isolated stimulus in protanope subjects was not detected in the ERG (Kremers et al., 2014; McKeefry et al., 2014), although there the responses are quite different in form (ON-responses are characterized by the presence of an a- and a b-wave, whereas OFF-responses show a d-wave). We believe the cortical interactions might be the cause of suppressing and or canceling the decrement signals.

This is also in contrast with psychophysical data where the sensitivity to OFF sawtooth stimuli was larger than to ON stimuli. The specific stimulus conditions (such as mean luminance) have large influence on psychophysical sensitivities to ON and OFF stimuli (Bowen, Pokorny, & Smith, 1989; Bowen, Pokorny, Smith, & Fowler, 1992). Possibly, the measured cortical responses are similarly influenced by mean luminance or other stimulus attributes. ERGs obtained varying the relative contrast show a linear relationship between the contrast and the response amplitudes (they were smaller for lower cone contrast stimuli) and the implicit times were not influenced by the cone contrast. It would be interesting to study in the future if this would also be the case with VEPs using cone-isolating stimuli.

VEP recording is a noninvasive clinical tool that can be easily and painlessly applied on verbal and nonverbal subjects, even in those with cognitive or motor impairment. However, VEPs show generally interindividual variability. As stated in the Results, we have also found individual variation of the signal that might provide difficulties if used in clinical testing. Despite the interindividual variability, the stimuli used in the present study provided consistent data. We propose that this protocol can be considered when investigating diseases that affect the visual system. Further investigation concerning the clinical application of the protocol is necessary. For instance, the deuteranopes showed different L_D profiles. The next step is to investigate the responses of more dichromats as well as anomalous trichromats.

Keywords: dichromat, color vision, silent substitution, visual evoked potential, visual pathways

Acknowledgements

This work was supported by Bundesministerium für Bildung und Forschung—BMBF (grant number 01DN14009 to JK); Conselho Nacional de Desenvolvimento Científico e Tecnológico—CNPq

(grant numbers 470785/2014-4 and 404239/2016-1 to MTSB, 456746/2014-5 to DMOB, and 490428/2013-4 to DFV); Coordenação de Aperfeiçoamento de Pessoal de Nível Superior—CAPES (grant number 3263/2013 to DFV); Deutsche Forschungsgemeinschaft (grant number KR1317/13-1 to JK); and Fundação de Amparo à Pesquisa do Estado de São Paulo (grant numbers 2016/22007-5 and 2016/04538-3 to MTSB, 2014/06457-5 to BVN, 2014/25743-9 to EH, and 2014/26818-2 to DFV). The authors would like to thank Neil Parry for comments on the manuscript.

Commercial relationships: none.

Corresponding author: Mirella Telles Salgueiro Barboni.

Email: mirellabarboni@usp.br.

Address: Department of Experimental Psychology, University of Sao Paulo, Brazil; and Department of Ophthalmology, Semmelweis University, Budapest, Hungary.

References

- American Clinical Neurophysiology Society. (2006). Guideline 5: Guidelines for standard electrode position nomenclature. *Journal of Clinical Neurophysiology*, 23, 107–110.
- Barboni, M. T. S., Nagy, B. V., Moura, A. L. A., Damico, F. M., Costa, M. F., Kremers, J., & Ventura, D. F. (2013). ON and OFF electroretinography and contrast sensitivity in Duchenne muscular dystrophy. *Investigative Ophthalmology and Visual Science*, 54, 3195–3204. [PubMed] [Article]
- Bowen, R. W., Pokorny, J., & Smith, V. C. (1989). Sawtooth contrast sensitivity: Decrements have the edge. *Vision Research*, 29(11): 1501–1509.
- Bowen, R. W., Pokorny, J., Smith, V. C., & Fowler, M. A. (1992). Sawtooth contrast sensitivity: Effects of mean illuminance and low temporal frequencies. *Vision Research*, 32(7), 1239–1247.
- Brainard, D. H., Roorda, A., Yamauchi, Y., Calderone, J. B., Metha, A., Neitz, M., . . . Jacobs, G. H. (2000). Functional consequences of the relative numbers of L and M cones. *Journal of the Optical Society of America A: Optics, Image Science, & Vision*, 17(3), 607–614.
- Derrington, A. M., Krauskopf, J., & Lennie, P. (1984). Chromatic mechanisms in lateral geniculate nucleus of macaque. *The Journal of Physiology*, 357, 241–265.
- DeValois, R. L., & DeValois, K. K. (1993). A multi-

- stage color model. *Vision Research*, 33(8), 1053–1065.
- Diller, L., Packer, O. S., Verweij, J., McMahon, M. J., Williams, D. R., & Dacey, D. M. (2004). L and M cone contributions to the midget and parasol ganglion cell receptive fields of macaque monkey retina. *Journal of Neuroscience*, 24(5), 1079–1088.
- Dow, B. M. (1974). Functional classes of cells and their laminar distribution in monkey visual cortex. *Journal of Neurophysiology*, 37(5), 927–946.
- Dow, B. M., & Gouras, P. (1973). Color and spatial specificity of single units in Rhesus monkey foveal striate cortex. *Journal of Neurophysiology*, 36(1), 79–100.
- Engel, S., Zhang, X., & Wandell, B. (1997). Colour tuning in human visual cortex measured with functional magnetic resonance imaging. *Nature*, 388(6637), 68–71.
- Estévez, O., & Spekreijse, H. (1974). A spectral compensation method for determining the flicker characteristics of the human colour mechanisms. *Vision Research*, 14, 823–830.
- Estévez, O., & Spekreijse, H. (1982). The “silent substitution” method in visual research. *Vision Research*, 22, 681–691.
- Giulianini, F., & Eskew, R. T. (1998). Chromatic masking in the (delta L/L, delta M/M) plane of cone-contrast space reveals only two detection mechanism. *Vision Research*, 38(24), 3913–3926.
- Gouras, P. (1970). Trichromatic mechanisms in single cortical neurons. *Science*, 168(3930), 489–492.
- Hall, T. A. (1999). BioEdit: A user-friendly biological sequence alignment editor and analysis program for Windows 95/98/NT. *Nucleic Acids Symposium Series*,(41), 95–98.
- Hubel, D. H., & Wiesel, T. N. (1966). Effects of varying stimulus size and color on single lateral geniculate cells in Rhesus monkeys. *Proceedings of the National Academy of Sciences, US*, 55(6), 1345–1346.
- Hubel, D. H., & Wiesel, T. N. (1968). Receptive fields and functional architecture of monkey striate cortex. *The Journal of Physiology*, 195, 215–243.
- Jacob, M. M., Pangeni, G., Gomes, B. D., Souza, G. S., Silva Filho, M., Silveira, L. C. L., ... Kremers, J. (2015). The spatial properties of L- and M-cone inputs to electroretinograms that reflect different types of post-receptoral processing. *PloS One*, 10, e0121218.
- Johnson, E. N., Hawken, M. J., & Shapley, R. (2001). The spatial transformation of color in the primary visual cortex of the macaque monkey. *Nature Neuroscience*, 4, 409–416.
- Kaneko, A. (1973). Receptive field organization of bipolar and amacrine cells in the goldfish retina. *The Journal of Physiology*, 235, 133–153.
- Kremers, J. (2003). The assessment of L- and M-cone specific electroretinographical signals in the normal and abnormal retina. *Progress in Retinal and Eye Research*, 22, 579–605.
- Kremers, J., Lee, B., & Kaiser, P. K. (1992). Sensitivity of macaque retinal ganglion cells and human observers to combined luminance and chromatic temporal modulation. *Journal of the Optical Society of America A: Optics and Image Science*, 9(9), 1477–1485.
- Kremers, J., & Pangeni, G. (2012). Electroretinographic responses to photoreceptor specific sine wave in modulation. *Journal of the Optical Society of America A: Optics, Image Science, & Vision*, 29(2), A306–A313, doi:10.1364/JOSAA.29.00A306.
- Kremers, J., Pangeni, G., Tsaousis, K. T., McKeefry, D., Murray, I. J., & Parry, N. R. (2014). Incremental and decremental L- and M-cone driven ERG responses: II. Sawtooth stimulation. *Journal of the Optical Society of America A: Optics and Image Science*, 31(4), A170–178.
- Kremers, J., Rodrigues, A. R., Silveira, L. C., & da Silva-Filho, M (2010). Flicker ERGs representing chromaticity and luminance signals. *Investigative Ophthalmology & Visual Science*, 51(1), 577–587. [PubMed] [Article]
- Lee, B. B., Martin, P. R., & Grünert, U. (2010). Retinal connectivity and primate vision. *Progress in Retinal and Eye Research*, 29(6): 622–639.
- Lennie, P., Krauskopf, J., & Sclar, G (1990). Chromatic mechanisms in striate cortex of macaque. *Journal of Neuroscience*, 10(2), 649–669.
- Maguire, J., Parry, N. R. A., Kremers, J., Kommanapalli, D., Murray, I. J., & McKeefry, D. J. (2016). Rod electroretinograms elicited by silent substitution stimuli from the light-adapted human eye. *Translational Vision Science & Technology*. 5(4):13, 1–14, doi:10.1167/tvst.5.4.13. [PubMed] [Article]
- McKeefry, D., Kremers, J., Kommanapalli, D., Challa, N. K., Murray, I. J., Maguire, J., & Parry, N. R. A. (2014). Incremental and decremental L- and M-cone driven ERG responses: I. Square-wave pulse stimulation. *Journal of the Optical Society of America A: Optics, Image Science, and Vision*, 31(4), A159–A169.
- Neitz, M., Carroll, J., Renner, A., Knau, H., Werner, J. S., & Neitz, J. (2004). Variety of genotypes in males diagnosed as dichromatic on a conventional clinical

- anomaloscope. *Visual Neuroscience*, 21(3), 205–216.
- Neitz, M., & Neitz, J. (1995). Numbers and ratios of visual pigment genes for normal red-green color vision. *Science*, 267(5200), 1013–1016.
- Pangeni, G., Lämmer, R., Tornow, R. P., Horn, F. K., & Kremers, J. (2012). On- and off-response ERGs elicited by sawtooth stimuli in normal subjects and glaucoma patients. *Documenta Ophthalmologica*, 124(3), 237–248.
- Parry, N. R., McKeefry, D. J., Kremers, J., & Murray, I. J. (2016). A dim view of M-cone onsets. *Journal of the Optical Society of America A: Optics, Image Science, and Vision*, 33(3), A207–213.
- Regan, B. C., Reffin, J. P., & Mollon, J. D. (1994). Luminance noise and the rapid determination of discrimination ellipses in colour deficiency. *Vision Research*, 34(10), 1279–1299.
- Rudvin, I., & Valberg, A. (2006). Flicker VEPs reflecting multiple rod and cone pathways. *Vision Research*, 46(5), 699–717.
- Sankeralli, M. J., & Mullen, K. T. (2001). Bipolar or rectified chromatic detection mechanisms? *Visual Neuroscience*, 18(1), 127–135.
- Smith, V. C., Lee, B. B., Pokorny, J., Martin, P. R., Valberg, A. (1992). Responses of macaque ganglion cells to the relative phase of heterochromatically modulated lights. *Journal of Physiology*, 458, 191–221.
- Tsai, T. I., Jacob, M. M., McKeefry, D., Murray, I. J., Parry, N. R., Kremers, J. (2016). Spatial properties of L- and M-cone driven incremental (On-) and decremental (Off-) electroretinograms: evidence for the involvement of multiple post-receptoral mechanisms. *Journal of the Optical Society of America A: Optics, Image Science, and Vision*, 33(3), A1–11.
- Werblin, F. S., & Dowling, J. E. (1969). Organization of the retina of the Mudpuppy, *Necturus maculosus*. II. Intracellular recording. *Journal of Neurophysiology*, 32, 339–355.
- Wiesel, T. N., & Hubel, D. H. (1966). Spatial and chromatic interactions in the lateral geniculate body of the rhesus monkey. *The Journal Neurophysiology*, 29(6), 1115–1156.
- Zeki, S. M. (1973). Colour coding in rhesus monkey prestriate cortex. *Brain Research*, 53(2), 422–427.